Annual Characteristics of a Passive Stack Ventilation System with Mechanically Controlled Air Supply Openings

Motoya Hayashi[1]
[1]Research Managing Director, National Institute of Public Health, Wako, Japan

Abstract

In order to retain good indoor air quality through the year in detached houses with passive ventilation systems, the author investigated a mechanical control air-supply method using a simulation program: "Fresh2015".

Fresh2015 simulates indoor environments in the houses with two types of structures and four types of ventilation systems. The simulation results showed that this mechanically controlled air-supply opening keeps ventilation rates adequate and makes the indoor air quality good from winter to the mild season especially in airtight houses.

Introduction

Passive ventilation systems (PVS) have been used in detached houses in Hokkaido, the coldest area of Japan, since 1990s. A benefit of PVS is that it does not need electrical energy for fans and its maintenance work is easy for the dwellers. The most beneficial point of PVS is that it keeps ventilation rates adequate without operation by dwellers, so it is a fail-safe system in retaining good indoor air quality in houses.

However, ventilation rates depend on weather conditions. Ventilation rates decrease in warm seasons. The lack of ventilation rates is a problem in most areas of Japan, and in 1999, a hybrid ventilation system (HVS) was developed using an electrical airflow sensor and a mechanical fan and it is widely used in Japan through the year. On the other hand, PVS is beginning to be used all over Japan as a ventilation system for winter.

In this study, a design method of retaining enough ventilation rates in houses with PVS in all seasons was investigated using a simulation program "Fresh2015".

Methods

In order to keep ventilation rates adequate in both winter and the mild seasons, a passive stack ventilation system using a mechanical dampers (TD) controlled by supply air temperature was designed. The system consists of a stack and an air supply route with a damper. The equivalent leakage area of TD changes with the temperature of supply air. This response of the equivalent leakage area toward the temperature of supply air has to be adjusted considering the weather conditions and the required ventilation rates. In order to develop an optimum method of retaining indoor air quality and at same time saving energy, the following studies were carried out. The author proposed an optimum method based on the weather conditions and the required ventilation rates.

1) Optimizing the temperature response of thermal damper TD

An airflow ratio of an air supply opening: a_1 is calculated from the airflow ratio of an exhaust opening: a_2 and the required airflow rate: Q_{req} as follows. The outdoor air pressure: Po is set to zero at the height of the air supply opening.

When n_1 is the same as n_2 ($n_1=n_2=n$), the following equations are obtained.

$$Q_{req} = a_1 \Delta p_1^{1/n} \quad (1)$$

$$-Q_{req} = -a_2(-\Delta p_2)^{1/n} \quad (2)$$

$$\Delta p_1 = -P_i \quad (3)$$

$$\Delta p_2 = (-h\rho_o)-(P_i-h\rho_i)=-P_i-h(\rho_o-\rho_i) \quad (4)$$

Where,

ρ_o: weight of outdoor air=$353/(273+\theta_o)$,
ρ_i: weight of indoor air=$353/(273+\theta_i)$,
θ_o: outdoor temperature,
θ_i: indoor air temperature

The next equation is obtained from equation 3 and equation1.

$$Q_{req} = a_1(-P_i)^{1/n} \quad (5)$$

The next equation is obtained from equation 4 and equation 2.

$$-Q_{req} = -a_2(P_i+h(\rho_o-\rho_i))^{1/n} \quad (6)$$

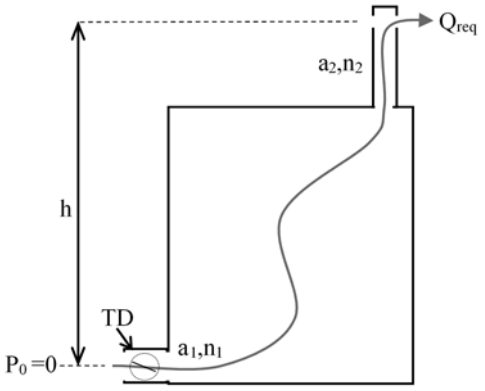

Figure 1 section of passive ventilation system

The next equation is obtained from equation 5 and equation 6.

$$Q_{req} = a_1(-P_i)^{1/n} = a_2(P_i+h(\rho_o-\rho_i))^{1/n} \quad (7)$$
$$\delta a_2(-P_i)^{1/n} = a_2(P_i+h(\rho_o-\rho_i))^{1/n} \quad (8)$$

Where, $\mu = a_1/a_2$

$$P_i = -h(\rho_o-\rho_i) \,/\, (1+\delta^n) \quad (9)$$

The next equation is obtained from equation 9 and equation 5.

$$Q_{req} = a_1(h(\rho_o-\rho_i) \,/\, (1+\delta^n))^{1/n} \quad (10)$$
$$Q_{req} = \delta a_2\,(h(\rho_o-\rho_i) \,/\, (1+\delta^n))^{1/n} \quad (11)$$
$$\mu = Q_n \,/\, (a_2{}^n h(\rho_o-\rho_i) - Q^n)^{-1/n} \quad (12)$$

Figure 2 shows the relationship between μ and the outdoor temperature. The ratio μ is the lowest in the case where n=2.0. Therefore, the air-supply opening area is small in this case.

2) Simulations using ”Fresh2015”

Airflow networks, indoor concentrations of pollutants (CO_2, HCHO) were calculated using leakage network models of Japanese wooden houses (an improved post-and-beam wooden structure and a wooden (2 inch x 4 inch) stud structure). The ventilation systems of simulated models were P (a passive ventilation system), TP (a passive ventilation system with TD) and mechanical ventilation systems (an exhaust and supply ventilation system and an exhaust ventilation system).Table 1 shows simulation models with several ventilation systems. In the case of TP, the required air supply rate (Q_{req}) is set to 120(m^3/h).

“Fresh” simulates the temperatures, the airflow rates, the concentrations and the generation rates of pollutants like formaldehyde: HCHO, carbon dioxide: CO_2 using the NHK standard living schedule model and the HASP weather data on Tokyo.
The simulation program was written in 1996, and was named ‘Fresh96‘. It was composed of the following three calculation methods.

① Dynamic thermal calculation of temperature, and heating and cooling loads.

Dr.Aratani devised the calculation method in 1974. The initial responses of the thermal-flow rates are calculated. The following equation was proposed in order to increase the speed of the calculation.

$$h(t) = B_0+\Sigma B_m e^{-\beta m \cdot t} + q \cdot \delta(t) \quad (13)$$

Where, $h(t)$ the initial response of thermal-flow rate, B_0 the steady value of thermal flow rate, $q=\Sigma B_m/\beta_m$ and $\delta(t)$ Delta function.

② Calculation of air flow rates in the multi-cell system

An equation of power at the openings: the airflow rates are calculated using the following equations which are led by the balances of power at openings is used.

$$[D]\{q^n\}+[K]\{\int qdt\}=\{F_{wind}\}+\{F_{temp}\}+\{F_{fan}\} \quad (14)$$

where q *the* airflow rate, n the exponent of airflow friction, $[D]$ the matrix of airflow friction, $[K]$ the matrix of room air elasticity, $\{F_{wind}\}$ the power of wind, $\{F_{temp}\}$ the power by the room air density $\{F_{fan}\}$ the power of fan.

③ Dynamic calculation of concentrations of pollutants

An equation of the amount of pollutants: the concentrations of pollutants in each room are calculated using the following equations which are led by the balance of the volume of the pollutants is used.

$$[Q]\{C(t)\}+[V]\{C'(t)\}=\{M(t)\} \quad (15)$$

where $[Q]$ the matrix of airflow rate $Q(i,j)$: the airflow rate from room-i to room-j, $Q(k,k)= -\Sigma_{k<>i}Q(k,i)$, $C(t)$

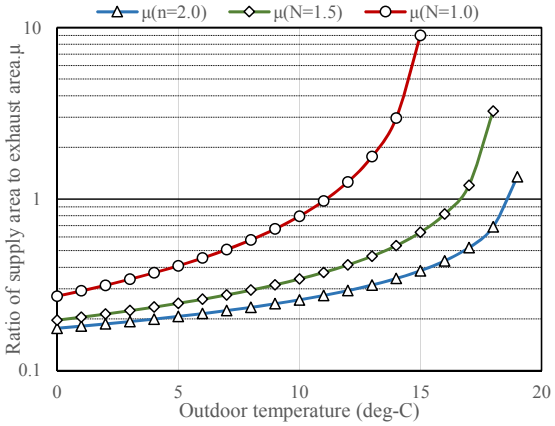

Figure 2 the response of air supply opening area to outdoor temperature

Table 1 Models for simulations

Type	E.R.A. of structure		Exhaust		Supply	
			h=8(m)	A.F.R./E.R.A.	h=0.5(m)	A.F.R./E.R.A.
A_ES	Wooden stud structure (2inchx4inch)	0.5 (cm^2/m^2)	Fan	120 (m^3/h)	Fan	120 (m^3/h)
A_E			Fan	120 (m^3/h)	O. at C.S.	247 (cm^2), n=2.0
A_P			Stack	313 (cm^2), n=2.0	O. at C.S.	247 (cm^2), n=2.0
A_TP			Stack	894 (cm^2)	O. at C.S.	120* (m^3/h)
B_ES	Improved post and beam structure	2.0 (cm^2/m^2)	Fan	120 (m^3/h)	Fan	120 (m^3/h)
B_E			Fan	120 (m^3/h)	O. at C.S.	247 (cm^2), n=2.0
B_P			Stack	313 (cm^2), n=2.0	O. at C.S.	247 (cm^2), n=2.0
B_TP			Stack	894 (cm^2), n=2.0	O. at C.S.	120* (m^3/h)

E.R.A: equivalent leakage area, A.F.R.: air flow rate, O.: opening, C.S.; clawl space,
* Q_{req}: required air flow rate

ES: exhaust and supply ventilation system, E: exhaust ventilation system, P: passive ventilation system,TP: passive ventilation system with thermal damper

the concentration of a pollutant, *[V]* the volume of rooms, *{M}* the emission rates of a pollutant in each room.

The equation can be solved using Newmark β numerical integration method. The emission rates of CO_2 are set using the average Japanese daily schedule and the data on the emission rates caused by the dwellers' behaviours in houses. The daily schedule of each family is set considering the plan of house. Figure 3 shows the calculated emission rates of CO_2. The emission rates of CO_2 are influenced by the behaviour of the family. The emission rates are high in the bedrooms on the second floor at night and the emission rates are high in the living room on the first floor at daytime. This is the pattern of the emission rates of CO_2 in a general Japanese detached house.
The emission rates of formaldehyde were calculated using an equation with the consideration of the influences of temperature and sink effect.

$$E = E_{25}(t) \cdot a^{(T-25)} - \beta \cdot C(t) \quad (16)$$

Where E: emission rate ($\mu g/(h \cdot m^2)$), E_{25} (=100 $\mu g/(h \cdot m^2)$): emission rate measured in small chamber when temperature is 25deg.C, T: temperature, a=1.11: measured in small chamber, β (= 0.06): ratio of sink measured in small chamber, C(t): concentration ($\mu g/m^3$)

E_{25} is influenced by the emission ability of building materials. The ability was supposed to be in proportion to the quantity of pollutant in material. Therefore, E_{25} is shown as the following equation.

$$E_{25}(t) = E_{25}(0) \cdot M(t)/M(0) \quad (17)$$

Where M(t): the quantity of pollutants in a material.

Initial formaldehyde emission rates in the concealed spaces are set to be 100 $\mu g/(h \cdot m^2)$ considering the surface area of emission sources like plywood. The concentration of carbon dioxide: CO_2 is set to be 400ppm.

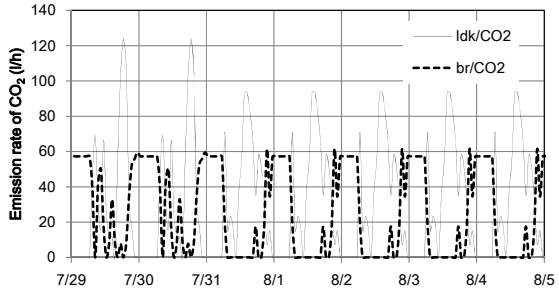

Figure 3 emission rates of CO_2 in a week

In this study, this program was improved by considering the effect of thermal damper according to the above equation 12.

Results

The indoor environments were simulated from February to March. Figure 4 and figure 5 shows the weather data of Tokyo. The outdoor temperature increases through this term and the temperature difference decrease and is close to zero in March. Therefore, the power of stack ventilation decreases in this term.

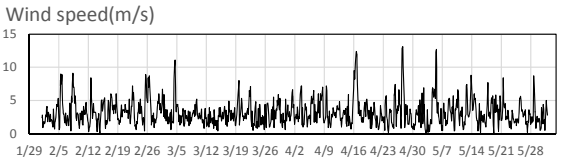

Figure 4 wind speed in Tokyo

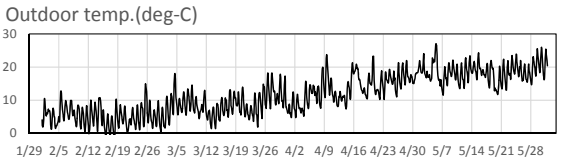

Figure 5 outdoor temperature in Tokyo

Figure 6 shows an airflow network of an airtight structure: A in the case of a passive ventilation: P in winter. Outdoor air is supplied to the crawl space and this air is divided to living spaces: ldk on the first floor and bedrooms: br on the second floor. The indoor air is exhausted from step and hall: sh and utility: ut through a stack.

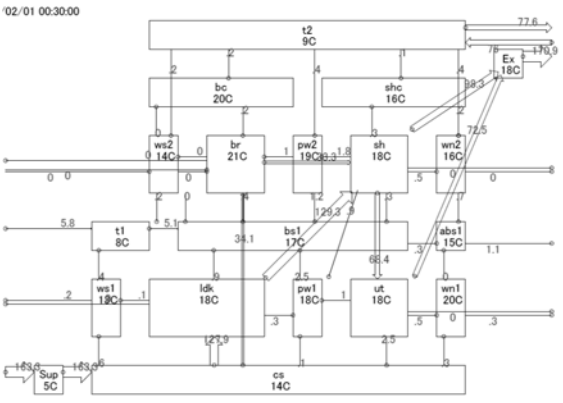

Figure 6 an airflow network of A_P

Figure 7 to 10 show the airflow rates of a supply opning and a exhaust opening in the case of the airtight structure: A. In the case of mechanical ventilation systems (figure 7 and 8), these airflow rates are almost steady. However the air supply rate fructuates a litlle in the case of an exhaust ventilation system: E in figure 8.
In the case of a passive ventilation system (figure 9), these airflow rate decrease in this term. The airflow rate fluctuates with the wind speed. This fructuation is more significant in the mild term than in winter.
In the case of a passive ventilation system with thermal damper: TP, the above mentiond trend of

outdoor temperatre is not significant as shown in figure 10. However the fructuation of wind speed is more significant than in the case of P. The opening area increaes with temperature rises and the influence of the wind upon these airflow rate increases.

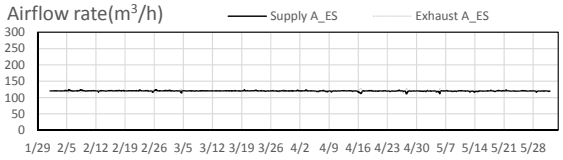

Figure 7 airflow rates of A_ES

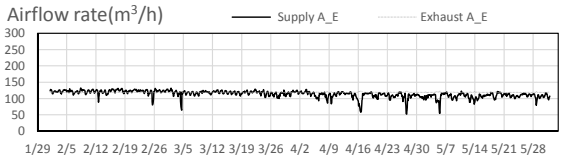

Figure 8 airflow rates of A_E

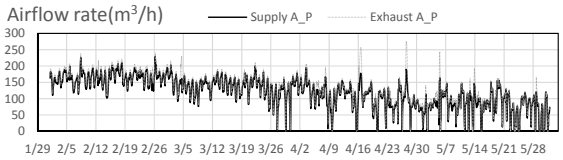

Figure 9 airflow rates of A_P

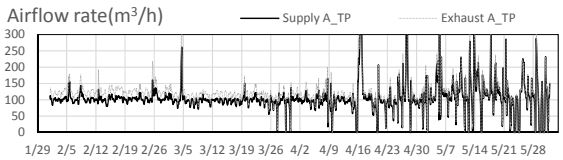

Figure 10 airflow rates of A_TP

Figure 11 to 14 show the indoor concentrations of CO_2 and HCHO in the case of airtight structure A. These concentrations are the averages of the concentrations in ldk and those in br. These concentrations depend on the airflow network and the emission rates. The CO_2 concentration changes daily with its emission rate as shown in figure 3. The emission rate of HCHO depends on the indoor temperature. Therefore, the HCHO emission rate increases gradually in this term.

In the cases of A_ES (figure 11), these concentrations are almost steady through this term. In the case of A_E (figure 12), these concentrations fluctuate and are sometimes higher than standard level (CO_2: 1000ppm, HCHO: 100 μg/m^3). This fluctuation depends on the airflow network. The airflow rate through br becomes low and the concentration becomes high. If the airflow design is improved, the fluctuation may be smaller.

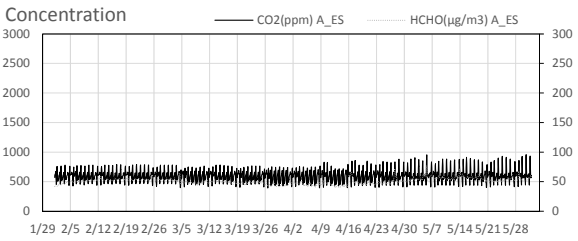

Figure 11 indoor concentrations of A_ES

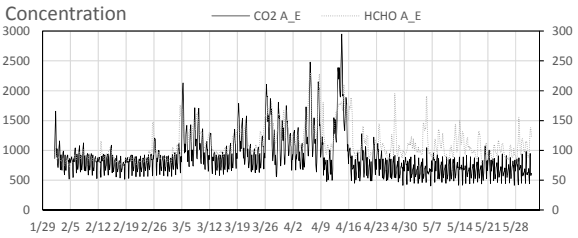

Figure 12 indoor concentrations of A_E

In the case of A_P (figure 13), these concentrations increase gradually with outdoor temperature. The trend is significant in the case of HCHO.

In the case of A_TP (figure 14), the above trend is not significant. These concentrations are low after April 16, when the air supply opening is large and the wind speed is high in this term.

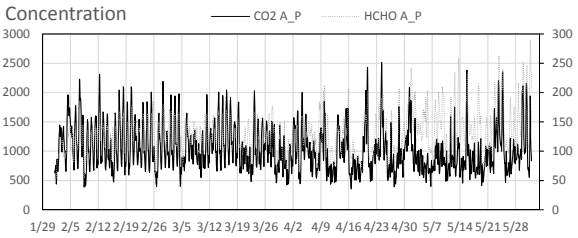

Figure 13 indoor concentrations of A_P

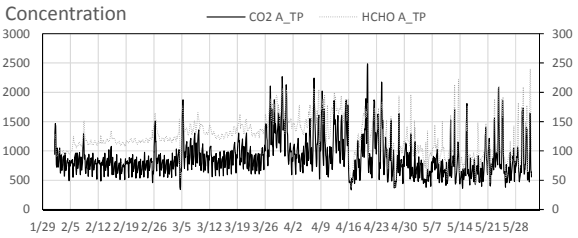

Figure 14 indoor concentrations of A_TP

Figure 15 to 18 show the relationship between outdoor temperature and airflow rates. In the case of mechanical ventilation systems A_ES and A_E (figure 15), the airflow rates do not depend on outdoor temperature. In the case of A_P (figure 16), the airflow rates depend on outdoor temperature. In the case of A_TP (figure 16), the airflow rates do not depend on outdoor temperature.

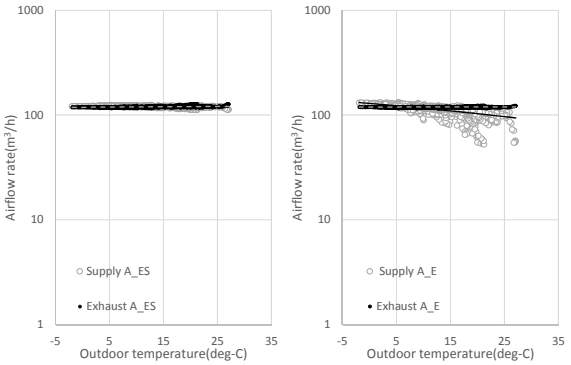

Figure 15 outdoor temperature and airflow rates in the case of A_ES and A_E

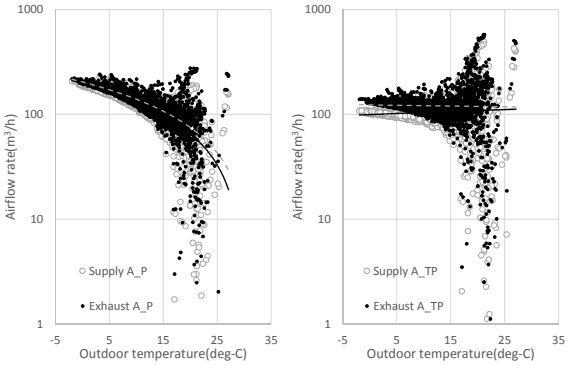

Figure 16 outdoor temperature and airflow rates in the case of A_P and A_TP

In the case of B_ES (figure17), the airflow rates do not depend on the outdoor temperature. In the case of B_E, outdoor temperature influences the air supply rate. In the case of B_P (figure18), the airflow rates depend on outdoor temperature. In the case of B_TP, the air supply rate does not depend on outdoor temperature. However, the outdoor temperature influences the exhaust rate.

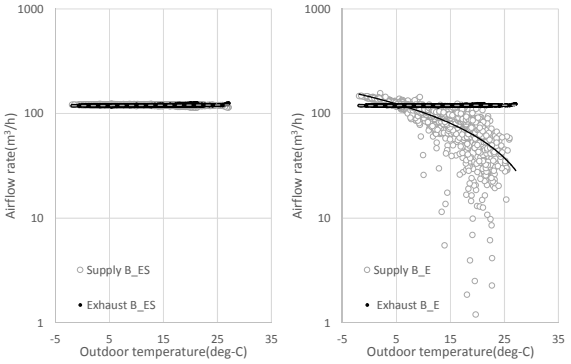

Figure 17 outdoor temperature and airflow rates in the case of B_ES and B_E

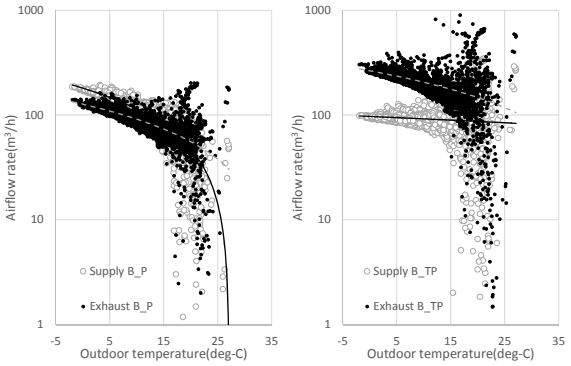

Figure 18 outdoor temperature and airflow rates in the case of B_P and B_TP

Figure 19 and 20 show the averages and standard deviations of airflow rates. The average of air supply rates is from 90 to 120 (m^3/h) as shown in figure 19. The average exhaust rate is 80 to 190 (m^3/h) as shown in figure 20. In the case of B_TP, the air exhaust rate is very large, because the infiltration rate is high in winter.

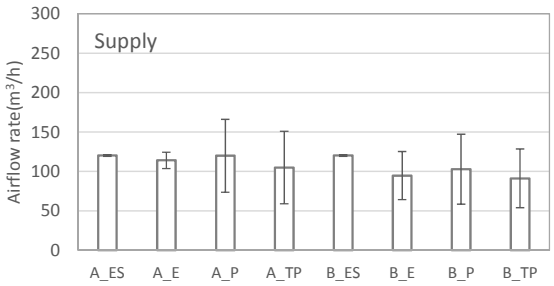

Figure 19 averages and standard deviations of air supply rates

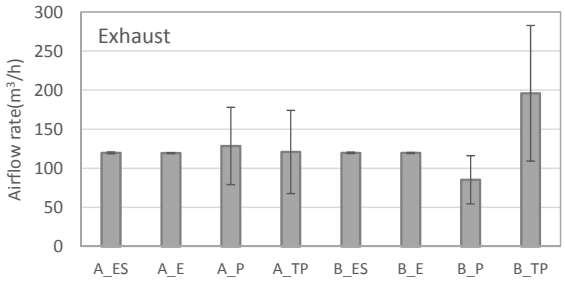

Figure 20 averages and standard deviations of air exhaust rates

Figure 21 and 22 show the averages and standard deviations of concentrations. The concentrations are higher in high airtight structures A than those in middle airtight structures B. The infiltration have an influence upon these low concentrations. The concentrations in ES is the lowest. The main factor of this comparison result is the airflow rates through the bedrooms: br. The concentrations are lower in TP than in P. The thermal damper has an effect on adequate indoor air concentrations.

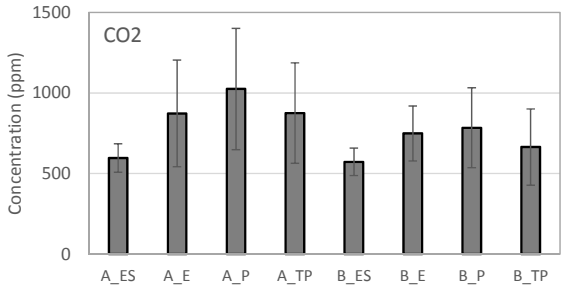

Figure 21 averages and standard deviations of indoor CO_2 concentrations

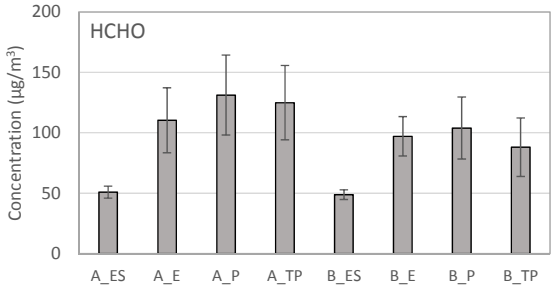

Figure 22 averages and standard deviations of indoor HCHO concentrations

Conclusion

The simulation results are as follows.

1) The airflow network and indoor concentrations of passive ventilation systems changes from winter to the mild season.
2) The indoor concentration depends on not only the airflow rate but also the leakage network.
3) In the case of passive ventilation, the design of airflow network is very important to retain good air quality.
4) Thermal dampers keep air supply rates almost steady and the effect is significant in airtight structures.

These studies showed a basic strategy to use passive ventilation not only in cold areas but also in mild areas in Japan.

Nomenclature

h(t)= the initial response of thermal-flow rate

B_0= the steady value of thermal-flow rate

δ (t)= Delta function

q = the airflow rate

n= the exponent of airflow friction

[D]= the matrix of airflow friction

[K]= the matrix of room air elasticity

$\{F_{wind}\}$= the power of wind

$\{F_{temp}\}$= the power by the room air density

[Q]= the matrix of airflow rate

Q(i,j)= the airflow rate from room-i to room-j

C(t)= the concentration of a pollutant

[V]= the volume of a room

{M}= the emission rate of a pollutant in each room.

Acknowledgements

"Grant-in-Aid Scientific Research of Japan Society for the Promotion of Science" supported this study.

References

NHK "The survey on the Japanese daily schedule 1990", Physiology Anthropology Institute of Japan, Handbook of Human Science Measurement, 1995.

N.Aratani,N.Sasaki,M.Enai,A Successive Integration Method for the Analysis of the Thermal Environment of Building, Building Science Series 39 of NBS, pp305-316, 1971

C.Y.Shaw and A.Kim 1984, "Performance of passive ventilation system in a two-story house" DBR Paper No.1276 October 1-4 p.11.1-11.27

M.Hayashi and H.Yamada 1996, "Performance of a passive ventilation system using beam space as a fresh_air supply chamber" Proc. of INDOOR AIR '96 Vol.1 859-864 JULY 21-261

M.Hayashi, H.Osawa, Y.Honma and M.Matsui, Prediction of air quality considering the concealed air leaks of houses, Proc.int.conf. " Building Simulation 2007",870-877.

M.Hayashi and H.Osawa, The influence of the concealed pollution sources upon the indoor air quality in houses, Building and Environment, Vol.43, Issue 3, March 2008, 329-336.

Motoya Hayashi and Haruki Osawa, Influence of the concealed air leaks upon the indoor Air Quality in Houses with prefabricated bathroom, Proc. of "Room vent 2009",505-512

Yoshinori Honma, M. Enai, A. Fukushima, H. Suzuki: The influence of airflow through leakage around floor on the hygrothermal conditions in a crawl space, Building Physics 2002 – 6th Nordic Symposium, pp.183-190, Trondheim, Norway

M.Hayashi,M.Enai,Y.Hirokawa, Annual Characteristics of Ventilation and Indoor Air Quality in Detached Houses using a Simulation Method with Japanese Daily Schedule Model, The International Journal of Building Science and its Applications BUILDING AND ENVIRONMENT Vol.36, pp.721-731,2001

M.Hayashi,H.Osawa,Prediction of Indoor Air Quality in Houses with Concentration-Control-Ventilation Systems Concidering the Concealed Air Leakes and Dwellers Opening Behavior, Proceedings of Building Simulation 2013